Author Manuscript

Author Manuscript

Author Manuscript

Author Manuscript

HHS Public Access

Author manuscript

Cell Rep. Author manuscript; available in PMC 2018 March 08.

Published in final edited form as:

Cell Rep. 2018 January 16; 22(3): 796–808. doi:10.1016/j.celrep.2017.12.078.

BRD4 Promotes DNA Repair and Mediates the Formation of TMPRSS2-ERG Gene Rearrangements in Prostate Cancer

Xiangyi Li[1,11], **GuemHee Baek**[1,11], **Susmita G. Ramanand**[1,11], **Adam Sharp**[2], **Yunpeng Gao**[1], **Wei Yuan**[2], **Jon Welti**[2], **Daniel N. Rodrigues**[2], **David Dolling**[3], **Ines Figueiredo**[2], **Semini Sumanasuriya**[2], **Mateus Crespo**[2], **Adam Aslam**[1], **Rui Li**[4], **Yi Yin**[4], **Bipasha Mukherjee**[5], **Mohammed Kanchwala**[6], **Ashley M. Hughes**[7], **Wendy S. Halsey**[7], **Cheng-Ming Chiang**[8,9,10], **Chao Xing**[6], **Ganesh V. Raj**[4], **Sandeep Burma**[5], **Johann de Bono**[2], and **Ram S. Mani**[1,4,8,12,*]

[1]Department of Pathology, UT Southwestern Medical Center, Dallas, TX 75390, USA

[2]Prostate Cancer Targeted Therapy and Cancer Biomarkers Group, Institute of Cancer Research and The Royal Marsden NHS Foundation Trust, Sutton, UK

[3]Clinical Trials and Statistics Unit, Institute of Cancer Research, London SM2 5NG, UK

[4]Department of Urology, UT Southwestern Medical Center, Dallas, TX 75390, USA

[5]Department of Radiation Oncology, UT Southwestern Medical Center, Dallas, TX 75390, USA

[6]Eugene McDermott Center for Human Growth & Development, UT Southwestern Medical Center, Dallas, TX 75390, USA

[7]Target Sciences, GlaxoSmithKline, Collegeville, PA 19426, USA

[8]Harold C. Simmons Comprehensive Cancer Center, UT Southwestern Medical Center, Dallas, TX 75390, USA

[9]Department of Biochemistry, UT Southwestern Medical Center, Dallas, TX 75390, USA

[10]Department of Pharmacology, UT Southwestern Medical Center, Dallas, TX 75390, USA

Summary

BRD4 belongs to the bromodomain and extraterminal (BET) family of chromatin reader proteins that bind acetylated histones and regulate gene expression. Pharmacological inhibition of BRD4 by BET inhibitors (BETi) has indicated antitumor activity against multiple cancer types. We show

This is an open access article under the CC BY-NC-ND license (http://creativecommons.org/licenses/by-nc-nd/4.0/).

*Correspondence: ram.mani@utsouthwestern.edu.
[11]Co-first author
[12]Lead Contact

Supplemental Information: Supplemental Information includes Supplemental Experimental Procedures, seven figures, and one table and can be found with this article online at https://doi.org/10.1016/j.celrep.2017.12.078.

Author Contributions: Conception and Design, R.S.M. and J.d.B.; Methodology Development, R.S.M., J.d.B., S.B., G.V.R., C.X., X.L., G.B., S.G.R., and A.S.; Data Acquisition, X.L., G.B., S.G.R., A.S., Y.G., W.Y., J.W., D.N.R., I.F., S.S., M.C., A.A., R.L., Y.Y., A.M.H., and W.S.H.; Data Analysis and Interpretation, X.L., G.B., S.G.R., A.S., Y.G., W.Y., J.W., D.N.R., D.D., S.S., R.L., Y.Y., M.K., C.X., G.V.R., S.B., J.d.B., and R.S.M.; Manuscript Writing, Review, and Revision, R.S.M with input from all authors; Administrative, Technical, or Material Support, B.M., M.K., C.-M.C., and C.X.; Study Supervision, R.S.M.

Declaration of Interests: The authors declare no competing interests.

Author Manuscript Author Manuscript Author Manuscript Author Manuscript

that BRD4 is essential for the repair of DNA double-strand breaks (DSBs) and mediates the formation of oncogenic gene rearrangements by engaging the non-homologous end joining (NHEJ) pathway. Mechanistically, genome-wide DNA breaks are associated with enhanced acetylation of histone H4, leading to BRD4 recruitment, and stable establishment of the DNA repair complex. In support of this, we also show that, in clinical tumor samples, BRD4 protein levels are negatively associated with outcome after prostate cancer (PCa) radiation therapy. Thus, in addition to regulating gene expression, BRD4 is also a central player in the repair of DNA DSBs, with significant implications for cancer therapy.

Graphical abstract

The classic function of BRD4 is to regulate gene expression. Li et al. present experimental and clinical data to suggest that BRD4 is also a key player in DNA repair and is associated with the development of CRPC after radiation therapy.

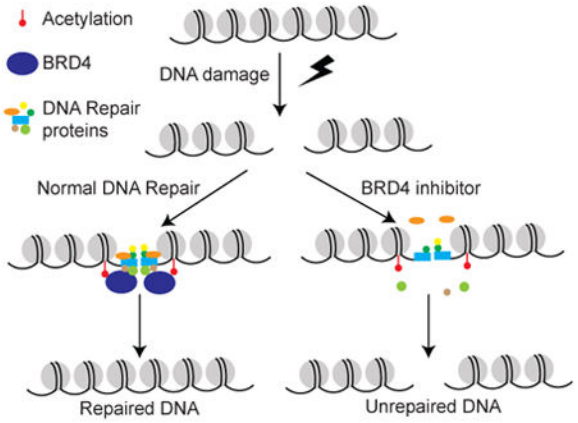

Introduction

Perturbations in the repair of DNA double-strand breaks (DSBs) contribute to the development of multiple cancers through the formation of oncogenic genomic rearrangements and other DNA lesions (Fröhling and Döhner, 2008; Mani and Chinnaiyan, 2010). For example, genomic rearrangements involving erythroblast transformation-specific (ETS) transcription factor family genes are considered driver events in prostate cancer (PCa) development. These rearrangements typically involve the fusion of androgen-regulated transcriptionally active genes with the ETS genes, resulting in the overexpression of the latter (Tomlins et al., 2005). The most prevalent ETS gene rearrangement, which is observed in >50% of PCas, involves the fusion of androgen receptor (AR) target gene, *TMPRSS2*, with the *ERG* proto-onco-gene, resulting in the formation of the *TMPRSS2-ERG* gene fusion. A combination of three-dimensional spatial proximity of the gene fusion partner loci and DNA breaks has been shown to promote the formation of gene fusions (Haffner et al., 2010; Lin et al., 2009; Mani et al., 2009, 2016). However, the DNA repair pathways and chromatin modifications underlying the formation of genomic rearrangements are far from clear.

Author Manuscript Author Manuscript Author Manuscript Author Manuscript

BRD4 belongs to the bromodomain and extraterminal (BET) family of reader proteins that translate signal-dependent chromatin alterations into gene expression readouts (Wu and Chiang, 2007). Preclinical studies have highlighted the impact of BET inhibitors (BETi) as potent anticancer agents. This has led to the development of clinical trials involving BET inhibitors as single agents or in combination with existing treatment options in multiple human cancers. Given the role of BRD4 in regulating histone acetylation-driven gene expression, it is generally believed that the anticancer effects of BETi is due to downregulation of BRD4 target genes like *MYC*, or by blunting the transcriptional output mediated by the androgen receptor (AR). However, downregulation of individual genes or gene signatures is insufficient to explain the magnitude of phenotypic effects conferred by BETi. For example, ectopic overexpression of MYC only partially rescues BETi-mediated inhibition of PCa cell growth; BETi being more effective than the AR inhibitor enzalutamide in blocking castration-resistant PCa (CRPC) development *in vivo* (Asangani et al., 2014; Wyce et al., 2013). Thus, BETi mediate their phenotypic effects by blocking additional pathways that are essential for cancer cell survival. As histone acetylation is associated both with gene expression regulation and DNA repair (Lee and Workman, 2007), we explored the role of BRD4 in the repair of DNA DSBs. In this paper, we present experimental and clinical data to suggest that BRD4 is a key mediator of NHEJ DNA repair pathway, promotes the formation of oncogenic gene fusions, and, importantly, is associated with PCa radiation therapy outcomes.

Results

BET Inhibition Regulates the Expression of DNA Repair Genes

We reasoned that histone acetylation-dependent, BRD4-mediated transcriptional regulation and DNA repair activity may be complementary. Thus, we conducted RNA sequencing (RNA-seq) experiments to study the gene expression changes in LNCaP cells upon BET inhibition with I-BET151. The downregulation of *MYC* expression in I-BET151-treated LNCaP cells served as a positive control for the experimental setup (Figure S1A). The expression levels of 7 out of 10 NHEJ pathway genes decreased upon treatment with I-BET151 (Figures 1A and 1B). The results of gene set enrichment analysis tests indicated that treatment with I-BET151 regulated the NHEJ pathway with near significance ($p = 0.08$). Consistent with the I-BET151 data, we observed that treatment with JQ1 (Filippakopoulos et al., 2010), the most commonly used BETi, also downregulated the expression of NHEJ DNA repair genes in two PCa cell lines (Figure S1B). We observed that small interfering RNA (siRNA)-based knockdown of BRD4, BRD2, or BRD3 resulted in the downregulation of many NHEJ DNA repair genes (Figure S2A). Simultaneous knockdown of all the three BET proteins was associated with maximal downregulation of NHEJ DNA repair genes in LNCaP and 22Rv1 cells, suggestive of functional redundancy among BET proteins. In addition, overexpression of BRD4 in LNCaP cells resulted in upregulation of the NHEJ DNA repair genes in a dose-dependent manner (Figure S2B). Given the observation that AR upregulates DNA repair genes (Goodwin et al., 2013; Polkinghorn et al., 2013), and BRD4 is essential for AR-dependent gene expression (Asangani et al., 2014), it is not surprising that BETi blocks the expression of DNA repair genes in prostate cells. To explore the clinical significance of this experimental approach, we conducted gene set enrichment analysis

Author Manuscript Author Manuscript Author Manuscript Author Manuscript

(GSEA) by mining BRD4 expression from RNA-seq datasets representing 122 CRPC patients from the SU2C cohort (Robinson et al., 2015). Remarkably, the 10 NHEJ pathway genes were significantly enriched and positively associated with BRD4 expression in clinical specimens (Figure 1C). Thus, we conclude that BRD4 regulates the expression of NHEJ DNA repair genes both in cell-based experimental models and CRPC clinical specimens.

The Role of BRD4 in NHEJ DNA Repair Pathway

As NHEJ DNA repair is the primary mediator of oncogenic genomic rearrangements, we explored the role of BRD4 in this pathway. We employed an engineered HEK293 cell line that expresses red fluorescent protein (RFP) only upon the repair of I-SceI endonuclease-induced DSBs by NHEJ (Mukherjee et al., 2012). The parental cells are GFP positive and RFP negative; transfection with an I-SceI expressing plasmid results in the formation of DSBs flanking the GFP gene (Figure 1D). The percentage of RFP positive cells following I-SceI transfection directly correlates with NHEJ activity in this assay. Treatment with JQ1 reduced the percentage of RFP positive cells in a dose-dependent manner, demonstrating inhibition of NHEJ DNA repair (Figures 1E and 1F). Consistent with this observation, BRD4 knockdown using siRNA also resulted in impaired NHEJ DNA repair (Figures 1G and S3A). These results indicated that BRD4 has an essential role in the general repair of DNA DSBs by NHEJ.

Next, we queried BRD4 transcript expression in The Cancer Genome Atlas (TCGA) primary PCa dataset (Cancer Genome Atlas Research Network, 2015). BRD4 expression was not significantly altered in PCa specimens when compared to normal prostate (Figure S3B). As ERG fusion positive and SPOP mutation positive specimens represent the two major, but mutually exclusive molecular subtypes of PCa, we reasoned that BRD4 may be differentially expressed in these molecular subtypes. BRD4 expression was significantly elevated in ERG fusion positive PCa specimens in comparison to either normal prostate or SPOP-mutated PCa specimens (Figure 1H); no significant changes in BRD4 expression was noted upon comparison of normal prostate and SPOP-mutated PCa. Thus, we conducted the next set of experiments to define the role of BRD4 in the formation of ERG gene rearrangements.

The Role of BRD4 in the Formation of Oncogenic *TMPRSS2-ERG* Gene Fusions

We employed CRISPR-Cas9 technology to induce *de novo TMPRSS2-ERG* gene fusions in androgen-responsive LNCaP cells, which lack these gene fusions. We hypothesized that co-transfection of single-guide RNAs (sgRNAs) targeting intron 1 of *TMPRSS2* and intron 3 of *ERG* would result in the simultaneous formation of Cas9-mediated DSBs in these two genes. While the cellular DNA repair machinery will fix most of these DNA DSBs, a subset of these breaks will inter-ligate to form *TMPRSS2-ERG* gene fusions (Figure 2A). We designed three different sgRNAs per gene and tested all the nine combinations for their ability to induce *TMPRSS2-ERG* gene fusions using TaqMan qRT-PCR assays. Seven of these nine sgRNA combinations induced the robust formation of *TMPRSS2-ERG* gene fusion RNA transcripts (Figure 2B). The T3 and E2 sgRNAs targeting *TMPRSS2* and *ERG*, respectively, were the most effective combinationin terms of gene fusion formation. Although all sgRNA combinations produced identical *TMPRSS2-ERG* fusion RNA transcript junctions, the genomic DNA junctions were unique for each sgRNA combination,

Author Manuscript Author Manuscript Author Manuscript Author Manuscript

as the DSBs are generated in different locations within the same introns. We developed a TaqMan qPCR assay to detect the predicted T3 and E2 sgRNA-induced *TMPRSS2-ERG* fusion genomic DNA junction. This assay was specific for the detection of fusions generated by the T3 and E2 sgRNA combination (Figure 2C). The CRISPR-Cas 9-induced genomic and transcript junctions were characterized by gel-based PCR, cloning, and sequencing (Figures 2D, 2E, S3C, and S3D). Importantly, the CRISPR-Cas9 system resulted in the formation of detectable levels of ERG protein in LNCaP cells. Moreover, consistent with the *TMPRSS2-ERG* fusion transcript data, the T3 and E2 sgRNA combination was associated with the maximal induction of ERG protein levels (Figure S3E). Thus, the CRISPR-Cas9 method allowed rapid, robust, and inducible formation of oncogenic gene fusions. We next employed the T3 and E2 sgRNA combination to identify mediators of gene fusion formation in subsequent experiments.

As the non-homologous end joining (NHEJ) DNA repair pathway is implicated in the formation of chromosomal translocations (Roukos and Misteli, 2014), we explored the role of this pathway in the formation of gene fusions. We studied the effect of knockdown of key NHEJ components such as PRKDC, PAXX, Artemis, KU70, KU80, XRCC4, LIG4, NHEJ1, XPF, 53BP1, and WRN in CRISPR-Cas9-mediated *TMPRSS2-ERG* gene fusion formation. As hypothesized, knockdown of individual NHEJ components blocked CRSPR-Cas9-mediated *TMPRSS2-ERG* gene fusion formation both in terms of fusion genomic DNA and fusion RNA transcript (Figures S3F, S3G, and S4A). Consistent with this observation, treatment with NU7026, a PRKDC inhibitor, blocked the formation of *TMPRSS2-ERG* gene fusions in a dose-dependent manner (Figures S4D and S4E). By recapitulating the role of NHEJ components, we validated the potential of our CRISPR-Cas9 assay to identify mediators of genomic rearrangements. This set the stage to discover novel regulators of genomic rearrangements.

We next tested the role of BRD4 in CRISPR-Cas9-mediated *TMPRSS2-ERG* gene fusion formation. BRD4 knockdown using four different siRNAs either individually or pooled, resulted in a significant block in *TMPRSS2-ERG* gene fusion formation, both in terms of fusion genomic DNA and fusion RNA transcript (Figures 2F, 2G, S4B, and S4C). Treatment with the BETi, JQ1, also blocked the formation of *TMPRSS2-ERG* gene fusions in a dose-dependent manner (Figures 2H and 2I). Thus, BRD4 is necessary for the formation of oncogenic *TMPRSS2-ERG* gene fusions, and possibly other genomic rearrangements as well.

BRD2 Promotes NHEJ DNA Repair and the Formation of Oncogenic TMPRSS2-ERG Gene Fusions

Analysis of RNA-seq data from the SU2C cohort revealed that the expression of *BRD4*, *BRD2*, and *BRD3* are correlated (Figure S5A). The endogenous expression of individual BET proteins was confirmed by immunoblot analysis in LNCaP cells (Figure S5B). BRD2 knockdown using siRNA also resulted in impaired NHEJ DNA repair (Figures 2J and S5C). These results indicated that BRD2 also promotes the repair of DNA DSBs by NHEJ. We tested the role of BRD2 in CRISPR-Cas9-mediated *TMPRSS2-ERG* gene fusion formation. BRD2 knockdown using multiple siRNAs either individually or pooled, resulted in a

Author Manuscript Author Manuscript Author Manuscript Author Manuscript

significant block in *TMPRSS2-ERG* gene fusion formation, both in terms of fusion genomic DNA and fusion RNA transcript (Figures 2K, 2L, and S5D). We conclude that BRD2 is also necessary for CRISPR-Cas9-induced *TMPRSS2-ERG* gene fusion formation.

Ionizing Radiation Induced DNA Damage-Dependent Genome-wide Acetylation of Histone H4

As acetylated histone H4 is the classic recognition target for BRD4 (Chiang, 2009), we hypothesized a DNA damage-induced, acetylation-dependent mechanism for recruitment of BRD4 to damaged chromosomes. Chromatin immunoprecipitation sequencing (ChIP-seq) experiments in LNCaP cells revealed that ionizing radiation (IR) treatment induced a significant, genome-wide increase in acetylation of histone H4 (Figures 3A–3C). Although we observed an increase in histone H4 acetylation in transcription start sites (TSSs) (Figure 3D), mainly at +1 nucleosome where BRD4 typically binds, this did not fully account for the substantial increase in genome-wide histone H4 acetylation upon IR treatment (cf. Figures 3C and 3D). As the primary effect of IR on chromatin is DNA damage, we reasoned that the enhanced histone H4 acetylation is likely to be directed to sites of DNA damage. DNase I hypersensitivity sites (DHSs) are hotspots for breaks; we have previously reported the involvement of DHSs in the formation of oxidative stress-induced *de novo* genomic rearrangements (Mani et al., 2016). Interestingly, we observed a significant increase in histone H4 acetylation in DHSs upon IR treatment (Figure 3E). The signature bi-modal peak is suggestive of nucleosome loss at the center of DHSs, which is associated with increased susceptibility to DNA breaks.

The prostate-specific transcriptionally active *TMPRSS2* locus has high levels of acetyl histone H4 at the TSS (Figure 3F, top). The first intron of *TMPRSS2*, a hotspot for DNA breaks, is the most frequently rearranged intron in PCa genomes as it fuses multiple ETS family genes, including *ERG*, to form the ETS gene fusions. We observed DHSs in the first intron of *TMPRSS2*. IR treatment induced significant acetylation of histone H4 in the first intron of *TMPRSS2*. These results suggest that DNA damage is associated with enhanced histone acetylation.

Homozygous deletions spanning the *PTEN* locus are observed in about 15% of primary PCas (Barbieri et al., 2012; Cancer Genome Atlas Research Network, 2015). The TSS of *PTEN* is enriched for the acetyl histone H4 mark (Figure 3F, bottom). We observed two IR-induced histone H4 acetylation sites near the 5′ and 3′ ends of the *PTEN* genes. One of these two acetylated sites is also a DHS, suggesting that the induced acetylation sites are hotspots for DNA breaks. We speculate that mis-repair of simultaneous DSBs at these induced acetylation sites could contribute to *PTEN* loss in PCa.

DNA Damage-Dependent Recruitment of BRD4 to Chromatin Results in Stable Establishment of the DNA Repair Complex

We conducted IR treatment and cell fractionation assays to further probe the role of acetylated histone H4 and BRD4 in the repair of DNA DSBs. Treatment of LNCaP cells with IR resulted in enhanced acetylation of histone H4 and increased recruitment of BRD4 to the chromatin fraction (Figure 4A, top). Co-immunoprecipitation experiments indicated

Author Manuscript Author Manuscript Author Manuscript Author Manuscript

that histone H4 acetylation mediated the recruitment of BRD4 to chromatin upon DNA damage (Figure 4A, bottom). γ-H2AX, representing phosphorylated histone H2AX (Ser139) was used as a positive control for DNA damage; H2AX and β-tubulin were employed as positive controls for chromatin and cytosolic fractions, respectively. Treatment with the BETi, JQ1, blocked the recruitment of BRD4 to the chromatin upon IR-induced DNA damage (Figure 4B).

Next, we hypothesized that, upon DNA damage, BRD4 interacts with additional DNA repair proteins, leading to their recruitment/stabilization, and the establishment of functional DNA repair complexes. BRD4 co-immunoprecipitated with several other proteins associated with DNA repair including 53BP1, KU80, KU70, and H2AX (Figure 4C). Acetylated histone H4, the primary recognition target for BRD4 was included as a positive control in these experiments; immunoglobulin G (IgG) was the negative control. The interaction of BRD4 with DNA repair proteins was further enhanced upon IR treatment. Thus, functional interactions between BRD4 and DNA repair proteins represent a potential mechanism for the role of BRD4 in NHEJ DNA repair.

We were intrigued by the interaction between the reader proteins BRD4 and 53BP1, which was significantly enhanced upon IR treatment. 53BP1 is a mediator of the DNA damage checkpoint (DiTullio et al., 2002; Fernandez-Capetillo et al., 2002; Wang et al., 2002), and, importantly, IR-induced 53BP1 foci formation is a hallmark of DNA damage response (DDR) signaling (Schultz et al., 2000). The BRD4-53BP1 interaction was confirmed by reverse co-immunoprecipitation experiments using both BRD4 and 53BP1 antibodies (Figure S6A). The results of proximity ligation assay (PLA) provided additional confirmation that IR treatment enhances the interaction between BRD4 and 53BP1 (Figures S6B and S6C).

We conducted the next set of experiments to explore the functional consequence of the interaction between BRD4 and 53BP1. Treatment with the BETi, JQ1, blocked the recruitment of 53BP1 to chromatin upon IR-induced DNA damage in LNCaP cells (Figure 4D). Similar results were obtained with siRNA-based BRD4 knockdown experiments (Figure S7A). Knockdown of 53BP1 did not block the recruitment of BRD4 to chromatin upon IR-induced DNA damage, suggesting BRD4 functions upstream of 53BP1 in the cascade of DNA repair events (Figure S7B). Given that both BRD4 and 53BP1 are reader proteins, we propose that BRD4 functions upstream in hierarchy and thus serves as a chromatin bookmark to guide the 53BP1 reader. Moreover, treatment with JQ1 blocked the recruitment of additional DNA repair proteins like Artemis and KU80 to the chromatin upon IR-induced DNA damage (Figure 4D). IR treatment did not affect the steady-steady expression of BET proteins or DNA repair proteins in LNCaP and 22Rv1 cells (Figure S7C). These results indicate that BRD4 is critical for stable formation of DNA repair complexes.

We extended our studies to dBET1, a next-generation BETi, synthesized by the conjugation of JQ1 with pthalimide moiety (Winter et al., 2015). dBET1 induces selective degradation of BET proteins. We observed that treatment with dBET1 blocked the IR-induced recruitment of BRD4, 53BP1, Artemis, KU80 and XRCC4 to the chromatin in two different cell line models—LNCaP and 22Rv1 (Figures 4E and 4F). Overall, therefore these results indicate

Author Manuscript Author Manuscript Author Manuscript Author Manuscript

that BRD4 participates in NHEJ DNA repair by (1) regulating the expression of NHEJ DNA repair genes, and (2) physically and functionally interacting with NHEJ DNA repair proteins, thereby contributing to the formation of stable DNA repair complexes, and resulting in efficient DNA repair.

Loss of BRD4 Function Enhances IR-Induced γ-H2AX Foci Formation

We next evaluated the effect of JQ1 and siRNA-based knockdown of BRD4 on IR-induced γ-H2AX foci formation in LNCaP cells. Treatment with JQ1 enhanced IR-induced γ-H2AX foci formation (Figures 5A and 5B). Consistent with this observation, BRD4 knockdown significantly enhanced IR-induced γ-H2AX foci formation (Figures 5C and 5D). Treatment with JQ1 or BRD4 knockdown in the absence of IR did not result in γ-H2AX foci formation. Interestingly, a high-throughput RNAi study has also identified BRD4 as a significant effector of IR-induced γ-H2AX foci formation (Floyd et al., 2013). Overall, these results indicate that absence of BRD4 results in defective repair of IR-induced DNA breaks.

BETi Synergizes with Enzalutamide to Enhance IR-Induced DNA Damage

We conducted comet assays to study the role of BRD4 in the restoration of genome integrity upon IR-induced DNA damage. IR treatment resulted in a dose-dependent increase in comet tail moment in LNCaP cells, indicating an increase in the proportion of unrepaired DNA breaks. BRD4 knockdown significantly enhanced IR-induced comet tail moment (Figures 6A and 6B). BRD4 knockdown in the absence of IR treatment did not increase comet tail moment, indicating that BRD4 loss does not contribute to the formation of DNA breaks per se, rather it modulates the downstream DNA repair events. Furthermore, these findings with BRD4 knockdown were recapitulated with pharmacological BETi by JQ1. The effects with JQ1 were more pronounced especially at low doses of IR treatment (Figure 6C and 6D). Since JQ1 targets multiple members of the BET family proteins, when compared to the siRNA, which only targets BRD4, it is reasonable to observe enhanced effects with JQ1.

We also conducted rescue experiments by overexpressing FLAG-tagged BRD4 in LNCaP cells. Treatment of LNCaP cells with IR resulted in enhanced recruitment of ectopically expressed FLAG-BRD4 to the chromatin fraction (Figure S7D). Remarkably, BRD4 overexpression led to a reduction in comet tail moment upon IR treatment, indicating a decrease in the proportion of unrepaired DNA breaks (Figure S7E). The results of these experiments clearly demonstrate an important role for BRD4 in the repair of DNA breaks.

Drugs targeting DNA repair including poly-(ADP)-ribose polymerase (PARP) inhibitors have been associated with anti-tumor activity in PCa subsets (Mateo et al., 2015). We next explored the utility of targeting DNA repair with BETi. The combination of androgen deprivation therapy (ADT) and radiation therapy (RT) is commonly used in the treatment of PCa. In patients with clinically lymphnode-positive PCa, compared with ADT alone, ADT +RT was associated with a decreased risk of 5-year all cause mortality (Lin et al., 2015). Likewise, compared to RT alone, RT + short-term ADT was associated with decreased PCa-specific mortality and increased overall survival (Jones et al., 2011). Mechanistically, ADT blocks AR-mediated DNA repair and thus improves the efficacy of RT (Goodwin et al.,

Author Manuscript Author Manuscript Author Manuscript Author Manuscript

2013; Polkinghorn et al., 2013; Spratt et al., 2015). Thus, we tested the effect of JQ1 and the AR antagonist, enzalutamide (as single agents or in combination) in IR-induced DNA damage (Figure 6E). Similar to our earlier result, JQ1 significantly increased IR-induced comet tail moment in LNCaP cells that endogenously express wild-type AR. Treatment of LNCaP cells with enzalutamide showed a small, but statistically non-significant increase of IR-induced comet tail moment. The combination of JQ1 and enzalutamide synergistically increased IR-induced comet tail moment in LNCaP cells (Figure 6E, left). We conducted this experiment in 22Rv1 cells that endogenously express both wild-type AR and a splice variant of AR that does not bind enzalutamide. Treatment with JQ1, but not enzalutamide, increased IR-induced comet tail moment in 22Rv1 cells. However, JQ1 did not synergize with enzalutamide to increase comet tail moment in 22Rv1 cells (Figure 6E, right). These results indicate that BETi can radiosensitize cells expressing AR splice variants that escape enzalutamide blockade.

Association of Nuclear BRD4 Protein Expression with the Development of CRPC after RT

To extend our discoveries to the clinical context, we optimized BRD4 protein immunohistochemistry (IHC) staining in formalin-fixed, paraffin-embedded (FFPE) PCa sections (Figure 7A). We next investigated the expression of BRD4 in prostate carcinogenesis and its association with primary treatment response. H-scores (HS) were determined by IHC and BRD4 antibody specificity was confirmed using BRD4 siRNA in LNCaP95 cells (Figure S7F). LNCaP95 is an androgen-independent and enzalutamide-resistant cell line derived from the parental LNCaP cells (Hu et al., 2012). We noticed higher BRD4 levels in LNCaP95 cells as compared to parental LNCaP cells (data not shown). We then compared BRD4 expression in clinical specimens representing normal prostate, prostatic intraepithelial neoplasia (PIN) and prostate adenocarcinoma (Figure 7B). Although variability in BRD4 protein expression was noted, we did not observe a statistically significant increase in BRD4 levels as patients developed prostate adenocarcinoma. This could be perhaps due to differential BRD4 expression in the various molecular subtypes of PCa (e.g., ERG fusion positive PCa versus SPOP mutation positive PCa) as suggested by our analysis of TCGA primary PCa data-set (Figures 1H and S3B).

As BETi have shown therapeutic activity in multiple pre-clinical models of cancer, we hypothesized that the inherent levels of variability in BRD4 levels may influence the outcome of treatments that primarily target genomic integrity (e.g., RT). Thus, we analyzed the expression of BRD4 in pre-treatment PCa biopsies of men who underwent primary therapy that included radical radiotherapy as part of their treatment paradigm. Higher nuclear BRD4 expression (continuous variable, per 100 HS) at diagnosis was significantly associated with shorter time to CRPC development after primary therapy (HR 6.7; 95% CI 1.5–31.0; $p = 0.01$). We divided the patient cohort by median nuclear BRD4 expression (BRD4 low, HS <100, 11 patients) and BRD4 high, HS ≥100, 17 patients). Patients in the high BRD4 group had significantly shorter median time to the development of CRPC compared to those in the low BRD4 group (2.8 [IQR 1.9–7.7] versus 9.1 [IQR 2.7–10.1] years, HR 3.9 [95% CI 1.4–10.9], $p = 0.01$; Figure 7C). There were no significant differences in the baseline characteristics between these patient groups (Table S1). Finally, we determined whether nuclear BRD4 expression was associated with overall survival in our

Author Manuscript Author Manuscript Author Manuscript Author Manuscript

patient cohort. Consistent with time to CRPC, higher nuclear BRD4 expression (continuous variable, per 100 HS) at diagnosis was associated with shorter overall survival (HR 5.5; 95% CI 1.0–29.7; p = 0.05). Although those patients in the high BRD4 group had a worse outcome compared to those in the low BRD4 group, this did not reach statistical significance (median 8.0 [IQR 5.1–13.5] versus 13.3 [IQR 7.9–13.8] years, HR 2.1 [0.8–5.5], p = 0.11; Figure 7D). Thus, pre-treatment nuclear BRD4 levels are associated with outcome from radical local RT for PCa.

Discussion

We demonstrate a novel role for BRD4 in the formation of oncogenic *TMPRSS2-ERG* fusions via its involvement in the NHEJ DNA repair pathway. Mechanistically, BRD4 is recruited to DNA DBSs by its interaction with acetylated histone H4, and perhaps other acetylated proteins. BRD4 also interacts with several DNA repair proteins; these interactions are further enhanced upon IR treatment. Given the role of BRD4 in gene regulation, it is not surprising that several DNA repair genes are mis-regulated upon treatment with BETi. We suggest that both the direct effects of BRD4 in orchestrating the response to IR or CRISPR-Cas9-induced DNA breaks, and these indirect effects by regulating the expression of DNA repair genes, are likely to be complementary.

We suggest that oncogenic gene fusions mirror many features of normal cellular processes like antibody gene rearrangements. BRD4 has been shown to promote class switch recombination (CSR) in B cells by facilitating the recruitment of 53BP1 to the switch regions (Stanlie et al., 2014). 53BP1 is essential for CSR in B lymphocytes (Manis et al., 2004; Ward et al., 2004). We suggest that DNA damage-induced cooperative interaction between BRD4 and 53BP1 promotes the formation of TMPRSS2-ERG gene fusions, presumably by (1) blocking DNA end resection (Bothmer et al., 2010), (2) promoting/maintaining synapsis of distal DNA elements (Difilippantonio et al., 2008), and (3) increasing chromatin mobility (Dimitrova et al., 2008). 53BP1 exhibits structural plasticity and can recognize at least two different histone marks: the dimethylated histone H4 lysine 20 (H4K20me2) (Botuyan et al., 2006; Sanders et al., 2004), and the histone H2A ubiquitinated on Lys 15 (H2AK15ub) (Fradet-Turcotte et al., 2013; Wilson et al., 2016). We speculate that BRD4 may guide 53BP1 to the damaged chromatin and thus serve as a reader's reader. Future studies should further refine our understanding of the nature, hierarchy, and origins of chromatin codes that are read by these reader proteins. BRD4 may also stabilize 53BP1 and the other DNA repair proteins at DSBs, leading to the formation of functional DNA repair complexes.

High-resolution mass spectrometry studies have identified lysine acetylation sites in several DNA repair proteins, including KU70 and KU80 (Choudhary et al., 2009). Thus, it is conceivable that the presence of two bromodomains help BRD4 and possibly other BET proteins to serve as adaptors to connect chromatin with acetylated DNA repair proteins. BRD4 may also promote acetylation-dependent cooperative interactions between DNA repair proteins leading to the establishment of multi-protein DNA repair complexes and liquid-liquid phase separation (Banani et al., 2017; Shin and Brangwynne, 2017). Such a model has been proposed for transcriptional regulation by super-enhancers (Hnisz et al.,

Author Manuscript Author Manuscript Author Manuscript Author Manuscript

2017). As BRD4 is a key component of super-enhancers, our study highlights common themes underlying the organization/regulation of super-enhancers and DNA repair complexes, and their vulnerability to BETi.

Our results also indicate that BET inhibition impairs the recruitment of 53BP1, Artemis, KU80, and potentially other DNA repair proteins to damaged chromatin. We also show that treatment with JQ1 enhanced IR-induced DNA damage and synergized with enzalutamide in cells expressing wild-type AR. Mechanistically, we show that these effects are due to targeting DNA repair. Since we also show that in clinical PCa samples, BRD4 protein expression is associated with outcome following radiotherapy, we now hypothesize that BETi can potentially be employed as a radiosensitizer in the radical treatment of higher risk localized PCas, especially in cancers with higher BRD4 expression.

Finally, our study demonstrates a new function for BRD4, a molecule that is widely implicated in the regulation of gene expression. Our results reposition BRD4 to the epicenter of DNA repair. These results are likely to enhance our understanding of cellular response to DNA damage and acquired resistance to cancer therapies that target DNA integrity, including RT and DNA-damaging anticancer drugs.

Experimental Procedures

Cell Culture and Transfection

LNCaP and 22Rv1 cells were obtained from American Type Culture Collection (ATCC) and cultured in RPMI 1640 medium containing 10% fetal bovine serum (FBS) in a 5% CO_2 humidified incubator. HEK293 cells were cultured in Eagle's Minimum Essential Medium containing 10% FBS. LNCaP95 cells were obtained from Alan K Meeker and Jun Luo (Johns Hopkins University, Baltimore, MD, USA). LNCaP95 cells were cultured in phenol red free RPMI 1640 medium supplemented with 10% charcoal-stripped FBS. All cell lines were verified by genotyping. Plasmid transfection was done using Lipofectamine® 3000 (Thermo Fisher Scientific, #L3000015) according to manufacturer's protocol. The pFLAG-CMV-BRD4 expression plasmid was a gift from Eric Verdin (Addgene plasmid #22304) (Bisgrove et al., 2007).

Patients and Tissue Samples

Patients with predominant areas of high-grade PIN and histologically normal prostate were identified from a population of men treated at UT Southwestern (UTSW) who underwent radical prostatectomy. UTSW patients provided written consent allowing the use of discarded surgical samples for research purposes according to an institutional board-approved protocol (STU-032011-187). De-identified patient samples were obtained from the UTSW Tissue Repository.

Patients were identified from a population of men treated at the Royal Marsden NHS Foundation Trust who received radical treatment for their PCa and went on to develop castration-resistant PCa (CRPC). Patients with a diagnosis of prostate adenocarcinoma with sufficient formalin-fixed, paraffin-embedded archival (diagnostic) tissue for BRD4 IHC were selected. Archival tissue was obtained from prostate needle biopsy (18), transurethral

Author Manuscript Author Manuscript Author Manuscript Author Manuscript

resection of the prostate (TURP; 2), or prostatectomy procedures (8). All tissue blocks were freshly sectioned and only considered for IHC analyses if adequate material was present (≥ 50 tumor cells; reviewed by D.N.R.). All patients had given written informed consent and were enrolled in institutional protocols approved by the Royal Marsden NHS Foundation Trust Hospital (London, UK) ethics review committee (reference no. 04/Q0801/60). A total of 28 patients had archival tissue sufficient for testing. Demographic and clinical data for each patient were retrospectively collected from the hospital electronic patient record system.

Tissue Analysis

IHC was performed using the rabbit anti-BRD4 antibody (Abcam; ab128874). Antigen retrieval was performed on slides in citrate buffer (pH 6.0) using a Menarini automated pressure cooker Menapath Antigen Access Unit. Anti-BRD4 antibody was diluted at 1:500 in Dako diluent and tissue was incubated for 1 hr. The reaction was visualized using the EnVison system. Cases were scored by a pathologist (D.N.R.) blinded to clinical data using the modified H score (HS) method; a semiquantitative assessment of staining intensity that reflects antigen concentration. HS was determined according to the formula: [(% of weak staining) × 1] + [(% of moderate staining) × 2] + [(% of strong staining) × 3], yielding a range from 0 to 300. Rabbit IgGs were used as a negative control. Cell pellets from LNCaP95 cells treated with BRD4 siRNA were used to confirm specificity of the antibody for BRD4.

Statistical Analysis

Time to CRPC was defined as the time from diagnosis (date of diagnostic biopsy unless clinical diagnosis was recorded as >1 month prior to biopsy) to documented progression (radiological, prostate-specific antigen [PSA], or change of treatment) on luteinizing hormone-releasing hormone (LHRH) agonist alone or with anti-androgen if started before/or with LHRH agonist. Overall survival was defined as time from diagnosis to date of death (21 patients) or last follow-up/contact (7 patients). Time-to-event end points (overall survival and time to CRPC) were assessed by means of Kaplan-Meier methods. Association with Nuclear BRD4 expression level was tested, as a continuous variable and dichotomized at the median HS of 100, using univariate Cox proportional hazards models. The proportional-hazards assumption was tested with the use of Schoenfeld residuals. Association between patient characteristics at diagnosis (age, PSA, Gleason score, and previous treatment) and nuclear BRD4 levels were tested using two-sample t test, Mann-Whitney U test, chi-square, and Fisher's exact test. Differences in nuclear BRD4 HS by cancer progression stage (normal, PIN, and adenocarcinoma) were assessed using the Kruskal-Wallis equality-of-populations rank test. All analyses were conducted using Stata v.13.1 and graphs were generated using GraphPad Prism v.6.

Data and Software Availability

The accession numbers for the ChIP-seq and RNA-seq data are GEO: GSE106258 and GSE103907, respectively.

Author Manuscript Author Manuscript Author Manuscript Author Manuscript

Supplementary Material

Refer to Web version on PubMed Central for supplementary material.

Acknowledgments

We thank M. Hardebeck and P. Todorova for technical assistance; B. Chen for the kind gift of Ku70 and Ku80 antibodies; A. Chinnaiyan, D. Castrillon, J. Malter, H. Sadek, and M.R.S. Rao for insightful comments and discussion; N. Safdar for manuscript edits. The authors acknowledge the assistance of the UT Southwestern Live Cell Imaging Facility, a Shared Resource of the Harold C. Simmons Cancer Center, is supported in part by an NCI Cancer Center Support Grant (1P30 CA142543-01). NIH Pathway to Independence (PI) Award (R00CA160640) to R.S.M. and startup funds from UT Southwestern supported research reported in this publication. R.S.M. also acknowledges funding from the ACS-IRG New Investigator Award in Cancer Research (IRG-02-196), and from the Prostate Cancer Research Program (PCRP) – Impact Award – US Department of Defense (W81XWH-17-1-0675). J.d.B. (W81XWH-17-1-0676) and G.V.R. (W81XWH-17-1-0674) acknowledges funding from the Prostate Cancer Research Program (PCRP) – Impact Award – US Department of Defense. The authors acknowledge funding from Prostate Cancer UK, the Prostate Cancer Foundation, Movember, Stand Up To Cancer, the US Department of Defense, Cancer Research UK, the UK Department of Health to the ICR/Royal Marsden ECMC, the Academy of Medical Sciences, and NHS funding to the NIHR Biomedical Research Centre at the Royal Marsden and The Institute of Cancer Research. A.S. is supported by a Medical Research Council fellowship. S.B. is supported by grants from the NIH (RO1CA149461, RO1CA197796, and R21CA202403) and the National Aeronautics and Space Administration (NNX16AD78G). C.-M.C. is supported by grants from the NIH (CA103867), CPRIT (RP140367), and the Welch Foundation (I-1805). C.X. was partially supported by NIH grant UL1TR001105.

References

Asangani IA, Dommeti VL, Wang X, Malik R, Cieslik M, Yang R, Escara-Wilke J, Wilder-Romans K, Dhanireddy S, Engelke C, et al. Therapeutic targeting of BET bromodomain proteins in castration-resistant prostate cancer. Nature. 2014; 510:278–282. [PubMed: 24759320]

Banani SF, Lee HO, Hyman AA, Rosen MK. Biomolecular condensates: Organizers of cellular biochemistry. Nat Rev Mol Cell Biol. 2017; 18:285–298. [PubMed: 28225081]

Barbieri CE, Baca SC, Lawrence MS, Demichelis F, Blattner M, Theurillat JP, White TA, Stojanov P, Van Allen E, Stransky N, et al. Exome sequencing identifies recurrent SPOP, FOXA1 and MED12 mutations in prostate cancer. Nat Genet. 2012; 44:685–689. [PubMed: 22610119]

Bisgrove DA, Mahmoudi T, Henklein P, Verdin E. Conserved P-TEFb-interacting domain of BRD4 inhibits HIV transcription. Proc Natl Acad Sci USA. 2007; 104:13690–13695. [PubMed: 17690245]

Bothmer A, Robbiani DF, Feldhahn N, Gazumyan A, Nussenzweig A, Nussenzweig MC. 53BP1 regulates DNA resection and the choice between classical and alternative end joining during class switch recombination. J Exp Med. 2010; 207:855–865. [PubMed: 20368578]

Botuyan MV, Lee J, Ward IM, Kim JE, Thompson JR, Chen J, Mer G. Structural basis for the methylation state-specific recognition of histone H4-K20 by 53BP1 and Crb2 in DNA repair. Cell. 2006; 127:1361–1373. [PubMed: 17190600]

Cancer Genome Atlas Research Network. The molecular taxonomy of primary prostate cancer. Cell. 2015; 163:1011–1025. [PubMed: 26544944]

Chiang CM. Brd4 engagement from chromatin targeting to transcriptional regulation: Selective contact with acetylated histone H3 and H4. F1000 Biol Rep. 2009; 1:98. [PubMed: 20495683]

Choudhary C, Kumar C, Gnad F, Nielsen ML, Rehman M, Walther TC, Olsen JV, Mann M. Lysine acetylation targets protein complexes and co-regulates major cellular functions. Science. 2009; 325:834–840. [PubMed: 19608861]

Difilippantonio S, Gapud E, Wong N, Huang CY, Mahowald G, Chen HT, Kruhlak MJ, Callen E, Livak F, Nussenzweig MC, et al. 53BP1 facilitates long-range DNA end-joining during V(D)J recombination. Nature. 2008; 456:529–533. [PubMed: 18931658]

Dimitrova N, Chen YC, Spector DL, de Lange T. 53BP1 promotes non-homologous end joining of telomeres by increasing chromatin mobility. Nature. 2008; 456:524–528. [PubMed: 18931659]

Author Manuscript Author Manuscript Author Manuscript Author Manuscript

DiTullio RA Jr, Mochan TA, Venere M, Bartkova J, Sehested M, Bartek J, Halazonetis TD. 53BP1 functions in an ATM-dependent checkpoint pathway that is constitutively activated in human cancer. Nat Cell Biol. 2002; 4:998–1002. [PubMed: 12447382]

Fernandez-Capetillo O, Chen HT, Celeste A, Ward I, Romanienko PJ, Morales JC, Naka K, Xia Z, Camerini-Otero RD, Motoyama N, et al. DNA damage-induced G2-M checkpoint activation by histone H2AX and 53BP1. Nat Cell Biol. 2002; 4:993–997. [PubMed: 12447390]

Filippakopoulos P, Qi J, Picaud S, Shen Y, Smith WB, Fedorov O, Morse EM, Keates T, Hickman TT, Felletar I, et al. Selective inhibition of BET bromodomains. Nature. 2010; 468:1067–1073. [PubMed: 20871596]

Floyd SR, Pacold ME, Huang Q, Clarke SM, Lam FC, Cannell IG, Bryson BD, Rameseder J, Lee MJ, Blake EJ, et al. The bromodomain protein Brd4 insulates chromatin from DNA damage signalling. Nature. 2013; 498:246–250. [PubMed: 23728299]

Fradet-Turcotte A, Canny MD, Escribano-Díaz C, Orthwein A, Leung CC, Huang H, Landry MC, Kitevski-LeBlanc J, Noordermeer SM, Sicheri F, Durocher D. 53BP1 is a reader of the DNA-damage-induced H2A Lys 15 ubiquitin mark. Nature. 2013; 499:50–54. [PubMed: 23760478]

Fröhling S, Döhner H. Chromosomal abnormalities in cancer. N Engl J Med. 2008; 359:722–734. [PubMed: 18703475]

Goodwin JF, Schiewer MJ, Dean JL, Schrecengost RS, de Leeuw R, Han S, Ma T, Den RB, Dicker AP, Feng FY, Knudsen KE. A hormone-DNA repair circuit governs the response to genotoxic insult. Cancer Discov. 2013; 3:1254–1271. [PubMed: 24027197]

Haffner MC, Aryee MJ, Toubaji A, Esopi DM, Albadine R, Gurel B, Isaacs WB, Bova GS, Liu W, Xu J, et al. Androgen-induced TOP2B-mediated double-strand breaks and prostate cancer gene rearrangements. Nat Genet. 2010; 42:668–675. [PubMed: 20601956]

Hnisz D, Shrinivas K, Young RA, Chakraborty AK, Sharp PA. A phase separation model for transcriptional control. Cell. 2017; 169:13–23. [PubMed: 28340338]

Hu R, Lu C, Mostaghel EA, Yegnasubramanian S, Gurel M, Tannahill C, Edwards J, Isaacs WB, Nelson PS, Bluemn E, et al. Distinct transcriptional programs mediated by the ligand-dependent full-length androgen receptor and its splice variants in castration-resistant prostate cancer. Cancer Res. 2012; 72:3457–3462. [PubMed: 22710436]

Jones CU, Hunt D, McGowan DG, Amin MB, Chetner MP, Bruner DW, Leibenhaut MH, Husain SM, Rotman M, Souhami L, et al. Radiotherapy and short-term androgen deprivation for localized prostate cancer. N Engl J Med. 2011; 365:107–118. [PubMed: 21751904]

Lee KK, Workman JL. Histone acetyltransferase complexes: One size doesn't fit all. Nat Rev Mol Cell Biol. 2007; 8:284–295. [PubMed: 17380162]

Lin C, Yang L, Tanasa B, Hutt K, Ju BG, Ohgi K, Zhang J, Rose DW, Fu XD, Glass CK, Rosenfeld MG. Nuclear receptor-induced chromosomal proximity and DNA breaks underlie specific translocations in cancer. Cell. 2009; 139:1069–1083. [PubMed: 19962179]

Lin, CC., Gray, PJ., Jemal, A., Efstathiou, JA. Androgen deprivation with or without radiation therapy for clinically node-positive prostate cancer. J Natl Cancer Inst. 2015. Published online July 23, 2015. https://doi.org/10.1093/jnci/djv200

Mani RS, Chinnaiyan AM. Triggers for genomic rearrangements: Insights into genomic, cellular and environmental influences. Nat Rev Genet. 2010; 11:819–829. [PubMed: 21045868]

Mani RS, Tomlins SA, Callahan K, Ghosh A, Nyati MK, Varambally S, Palanisamy N, Chinnaiyan AM. Induced chromosomal proximity and gene fusions in prostate cancer. Science. 2009; 326:1230. [PubMed: 19933109]

Mani RS, Amin MA, Li X, Kalyana-Sundaram S, Veeneman BA, Wang L, Ghosh A, Aslam A, Ramanand SG, Rabquer BJ, et al. Inflammation-induced oxidative stress mediates gene fusion formation in prostate cancer. Cell Rep. 2016; 17:2620–2631. [PubMed: 27926866]

Manis JP, Morales JC, Xia Z, Kutok JL, Alt FW, Carpenter PB. 53BP1 links DNA damage-response pathways to immunoglobulin heavy chain class-switch recombination. Nat Immunol. 2004; 5:481–487. [PubMed: 15077110]

Mateo J, Carreira S, Sandhu S, Miranda S, Mossop H, Perez-Lopez R, Nava Rodrigues D, Robinson D, Omlin A, Tunariu N, et al. DNA-repair defects and olaparib in metastatic prostate cancer. N Engl J Med. 2015; 373:1697–1708. [PubMed: 26510020]

Author Manuscript Author Manuscript Author Manuscript Author Manuscript

Mukherjee B, Tomimatsu N, Amancherla K, Camacho CV, Pichamoorthy N, Burma S. The dual PI3K/mTOR inhibitor NVP-BEZ235 is a potent inhibitor of ATM- and DNA-PKCs-mediated DNA damage responses. Neoplasia. 2012; 14:34–43. [PubMed: 22355272]

Polkinghorn WR, Parker JS, Lee MX, Kass EM, Spratt DE, Iaquinta PJ, Arora VK, Yen WF, Cai L, Zheng D, et al. Androgen receptor signaling regulates DNA repair in prostate cancers. Cancer Discov. 2013; 3:1245–1253. [PubMed: 24027196]

Robinson D, Van Allen EM, Wu YM, Schultz N, Lonigro RJ, Mosquera JM, Montgomery B, Taplin ME, Pritchard CC, Attard G, et al. Integrative clinical genomics of advanced prostate cancer. Cell. 2015; 161:1215–1228. [PubMed: 26000489]

Roukos V, Misteli T. The biogenesis of chromosome translocations. Nat Cell Biol. 2014; 16:293–300. [PubMed: 24691255]

Sanders SL, Portoso M, Mata J, Bähler J, Allshire RC, Kouzarides T. Methylation of histone H4 lysine 20 controls recruitment of Crb2 to sites of DNA damage. Cell. 2004; 119:603–614. [PubMed: 15550243]

Schultz LB, Chehab NH, Malikzay A, Halazonetis TD. p53 binding protein 1 (53BP1) is an early participant in the cellular response to DNA double-strand breaks. J Cell Biol. 2000; 151:1381–1390. [PubMed: 11134068]

Shin, Y., Brangwynne, CP. Liquid phase condensation in cell physiology and disease. Science. 2017. Published online September 22, 2017. https://doi.org/10.1126/science.aaf4382

Spratt DE, Evans MJ, Davis BJ, Doran MG, Lee MX, Shah N, Wong-vipat J, Carnazza KE, Klee GG, Polkinghorn W, et al. Androgen receptor upregulation mediates radioresistance after ionizing radiation. Cancer Res. 2015; 75:4688–4696. [PubMed: 26432404]

Stanlie A, Yousif AS, Akiyama H, Honjo T, Begum NA. Chromatin reader Brd4 functions in Ig class switching as a repair complex adaptor of nonhomologous end-joining. Mol Cell. 2014; 55:97–110. [PubMed: 24954901]

Tomlins SA, Rhodes DR, Perner S, Dhanasekaran SM, Mehra R, Sun XW, Varambally S, Cao X, Tchinda J, Kuefer R, et al. Recurrent fusion of TMPRSS2 and ETS transcription factor genes in prostate cancer. Science. 2005; 310:644–648. [PubMed: 16254181]

Wang B, Matsuoka S, Carpenter PB, Elledge SJ. 53BP1, a mediator of the DNA damage checkpoint. Science. 2002; 298:1435–1438. [PubMed: 12364621]

Ward IM, Reina-San-Martin B, Olaru A, Minn K, Tamada K, Lau JS, Cascalho M, Chen L, Nussenzweig A, Livak F, et al. 53BP1 is required for class switch recombination. J Cell Biol. 2004; 165:459–464. [PubMed: 15159415]

Wilson MD, Benlekbir S, Fradet-Turcotte A, Sherker A, Julien JP, McEwan A, Noordermeer SM, Sicheri F, Rubinstein JL, Durocher D. The structural basis of modified nucleosome recognition by 53BP1. Nature. 2016; 536:100–103. [PubMed: 27462807]

Winter GE, Buckley DL, Paulk J, Roberts JM, Souza A, Dhe-Paganon S, Bradner JE. DRUG DEVELOPMENT. Phthalimide conjugation as a strategy for in vivo target protein degradation. Science. 2015; 348:1376–1381. [PubMed: 25999370]

Wu SY, Chiang CM. The double bromodomain-containing chromatin adaptor Brd4 and transcriptional regulation. J Biol Chem. 2007; 282:13141–13145. [PubMed: 17329240]

Wyce A, Degenhardt Y, Bai Y, Le B, Korenchuk S, Crouthame MC, McHugh CF, Vessella R, Creasy CL, Tummino PJ, Barbash O. Inhibition of BET bromodomain proteins as a therapeutic approach in prostate cancer. Oncotarget. 2013; 4:2419–2429. [PubMed: 24293458]

Author Manuscript Author Manuscript Author Manuscript Author Manuscript

Highlights

- BRD4 promotes NHEJ DNA repair and regulates the expression of DNA repair genes
- BRD4 mediates the formation of TMPRSS2-ERG gene fusions in prostate cancer
- DNA-damage-induced histone H4 acetylation recruits BRD4 to chromatin
- BRD4 expression is associated with the development of CRPC after radiation therapy

Author Manuscript Author Manuscript Author Manuscript Author Manuscript

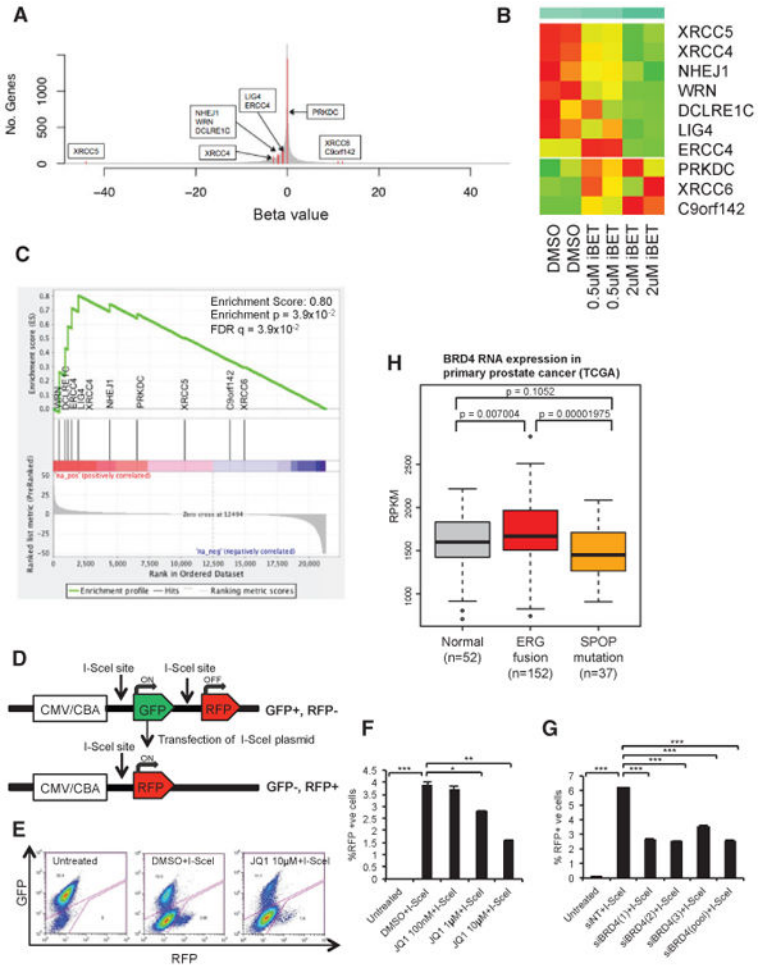

Figure 1. Regulation of DNA Repair Genes and NHEJ DNA Repair by BET Inhibitors

(A) Histogram representation of beta values indicating gene expression (from RNA-seq experiment) upon treatment of LNCaP cells with I-BET151 for 8 hr. Red colored bars represent 10 NHEJ genes.

(B) Heatmap representation of the expression of DNA repair genes (from RNA-seq experiment) upon treatment of LNCaP cells with the indicated doses of I-BET151.

(C) Gene set enrichment analysis (GSEA) of *BRD4* expression level from castration-resistant PCa (CRPC) specimens (n = 122) against the 10 NHEJ DNA repair genes.

(D) Schematic of the NHEJ DNA repair assay.

(E) Representative flow cytometry profiles to describe the effects JQ1 on the repair of I-SceI-induced DNA DSBs by the NHEJ pathway.

(F and G) Quantitative analysis of the effects of JQ1 (F) or siRNA against *BRD4* (G) on the repair of I-SceI-induced DNA DSBs by the NHEJ pathway (*p < 0.05; **p < 0.01; ***p < 0.001 by two-tailed Student's t test; error bars, SD of 3 technicalreplicates).

(H) BRD4 RNA expression in normal prostate, ERG fusion positive and SPOP mutant primary prostate adenocarcinoma samples from TCGA dataset.

Author Manuscript Author Manuscript Author Manuscript Author Manuscript

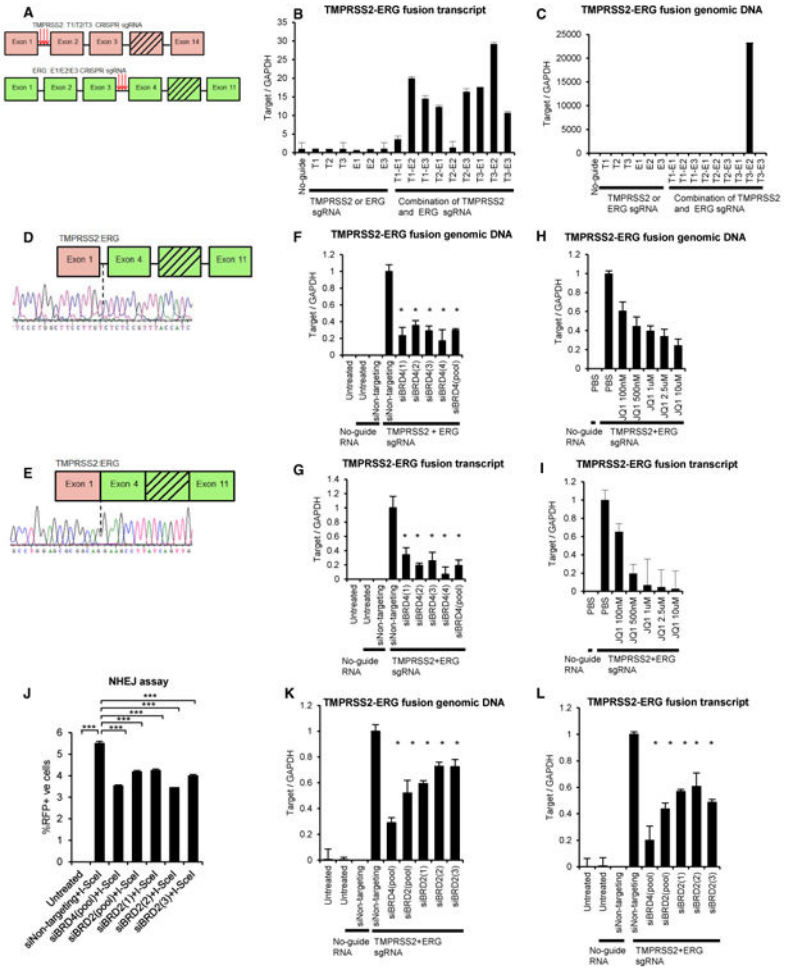

Figure 2. BRD4 Promotes *TMPRSS2-ERG* Genomic Rearrangements

(A) Schematic representation of the CRISPR-Cas9 assay to engineer *TMPRSS2-ERG* genomic rearrangements. The single-guide RNA (sgRNA) target sites in the introns of *TMPRSS2* and *ERG* genes are indicated by red arrows.

(B) A TaqMan qRT-PCR assay to detect *TMPRSS2-ERG* fusion RNA transcripts. T1, T2, and T3 represent sgRNAs that target the *TMPRSS2* locus; E1, E2, and E3 represent sgRNAs that target the *ERG* locus.

(C) A TaqMan quantitative qPCR assay to detect the specific *TMPRSS2-ERG* fusion genomic DNA junction induced by combination treatment with T3 and E2 sgRNAs.

(D) Sequence analysis of TMPRSS2-ERG fusion genomic DNA junction in LNCaP cells obtained by combination treatment with T3 and E2 sgRNAs. Gene structures for *TMPRSS2* and *ERG* are shown using the GenBank reference sequences NM_005656 and NM_004449, respectively.

(E) Sequence analysis of *TMPRSS2-ERG* fusion transcript junction in LNCaP cells obtained by combination treatment with T3 and E2 sgRNAs.

(F and G) TaqMan qPCR assay to detect the specific *TMPRSS2-ERG* fusion genomic DNA junction (F) or TaqMan-qRT-PCR assay for RNA transcript junction (G) in LNCaP cells treated with siRNA against *BRD4*, in combination with sgRNAs targeting *TMPRSS2* and

Author Manuscript Author Manuscript Author Manuscript Author Manuscript

ERG genes. siBRD4 (pool) represents combination of the four-individual siRNAs against BRD4 (*p < 0.001 by two-tailed Student's t test; error bars, SD of 3 technical replicates).
(H and I) TaqMan qPCR assay to detect the specific *TMPRSS2-ERG* fusion genomic DNA junction (H) or TaqMan-qRT-PCR assay for RNA transcript junction (I) in LNCaP cells treated with various doses of JQ1, in combination with sgRNAs targeting *TMPRSS2* and *ERG* genes.
(J) Quantitative analysis of the effects of siRNA against *BRD2* on the repair of I-SceI-induced DNA DSBs by the NHEJ pathway (***p < 0.001 by two-tailed Student's t test; error bars, SD of 3 technical replicates).
(K and L) TaqMan qPCR assay to detect the specific *TMPRSS2-ERG* fusion genomic DNA junction (K) or TaqMan-qRT-PCR assay for RNA transcript junction (L) in LNCaP cells treated with siRNA against *BRD2*, in combination with sgRNAs targeting *TMPRSS2* and *ERG* genes. siBRD2 (pool) represents combination of the four individual siRNAs against BRD2 (*p < 0.001 by two-tailed Student's t test; error bars, SD of 3 technical replicates).

Author Manuscript Author Manuscript Author Manuscript Author Manuscript

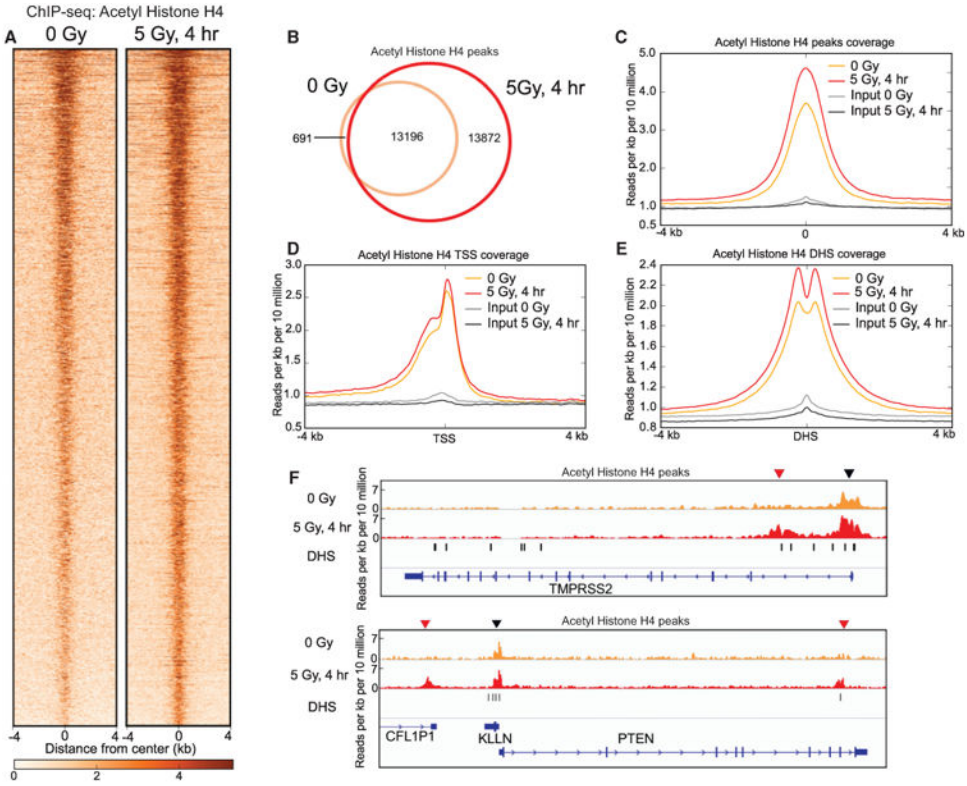

Figure 3. Ionizing Radiation Induces Acetylation of Histone H4 in the Chromatin

(A) Heatmap representation of ChIP-seq signals ±4 kb around Acetyl histone H4 peaks in LNCaP cells treated with or without 5 Gy IR. Samples were processed 4 hr post-treatment. The heatmaps are paired and sorted by the 0-Gy treatment.

(B) Venn diagram representing acetyl histone H4 peaks in untreated or 5-Gy IR-treated LNCaP cells.

(C–E) Average coverage plots showing enrichment of Acetyl histone H4 genome-wide (C), at transcription start sites (TSS) (D) and DNase I hypersensitivity sites (DHSs) (E).

(F) Genome browser representation of Acetyl histone H4 peaks in *TMPRSS2* and *PTEN* genes. Black triangles represent common peaks and red triangles represent IR-induced peaks.

Author Manuscript Author Manuscript Author Manuscript Author Manuscript

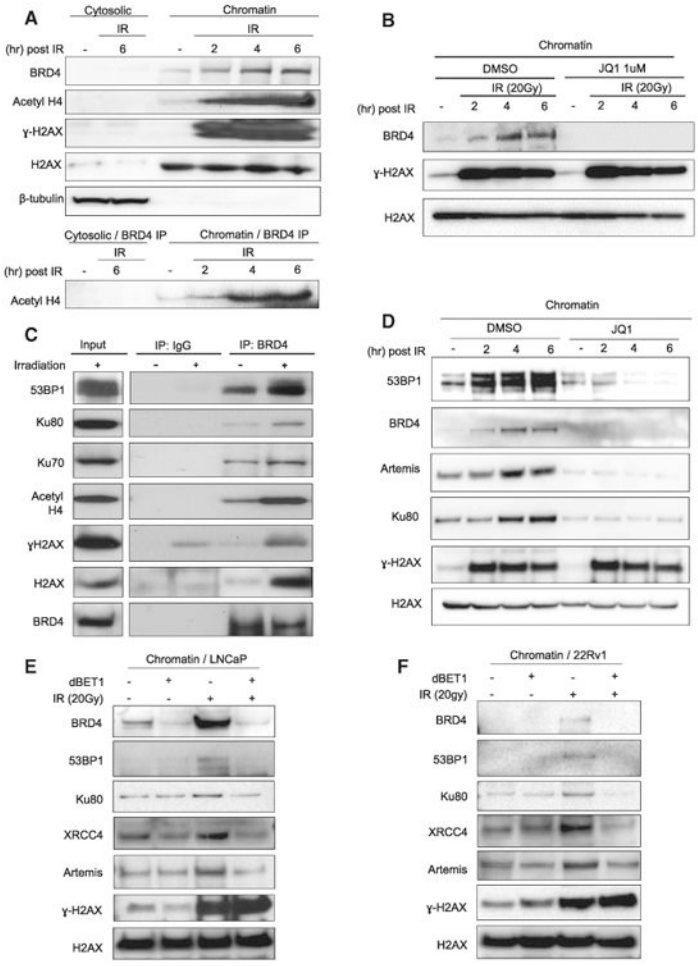

Figure 4. BRD4 Is Recruited to the Chromatin upon DNA Damage and Functionally Interacts with DNA Repair Proteins

(A) Histone H4 acetylation and BRD4 recruitment to the chromatin upon ionizing radiation (IR)-induced DNA damage (20 Gy) in LNCaP cells (top). γ-H2AX is the positive control for IR treatment; H2AX serves as positive control for the chromatin fraction and negative control for cytosolic fraction; β-tubulin serves as positive control for cytosolic fraction and negative control for chromatin fraction. BRD4 was immunoprecipitated from the same lysates and analyzed by immunoblot using anti-acetyl histone H4 antibody (bottom).

(B) The role of JQ1 in recruitment of BRD4 to the chromatin upon IR-induced DNA damage (20 Gy) in LNCaP cells.

(C) Co-immunoprecipitation (Co-IP) experiments with nuclear extracts from untreated or IR-treated LNCaP cells (20 Gy). 1 hr post-IR treatment, the immunoprecipitation (IP) was performed using anti-BRD4 antibody and analyzed by immunoblot with the indicated antibodies.

(D) The role of JQ1 (10 μM) in the recruitment of BRD4, 53BP1, Artemis, and Ku80 to the chromatin upon IR-induced DNA damage (20 Gy) in LNCaP cells.

(E and F) The role of dBET1 (1 μM) in the recruitment of BRD4 and DNA repair proteins to the chromatin upon IR-induced DNA damage in LNCaP (E) and 22Rv1 cells (F).

Author Manuscript Author Manuscript Author Manuscript Author Manuscript

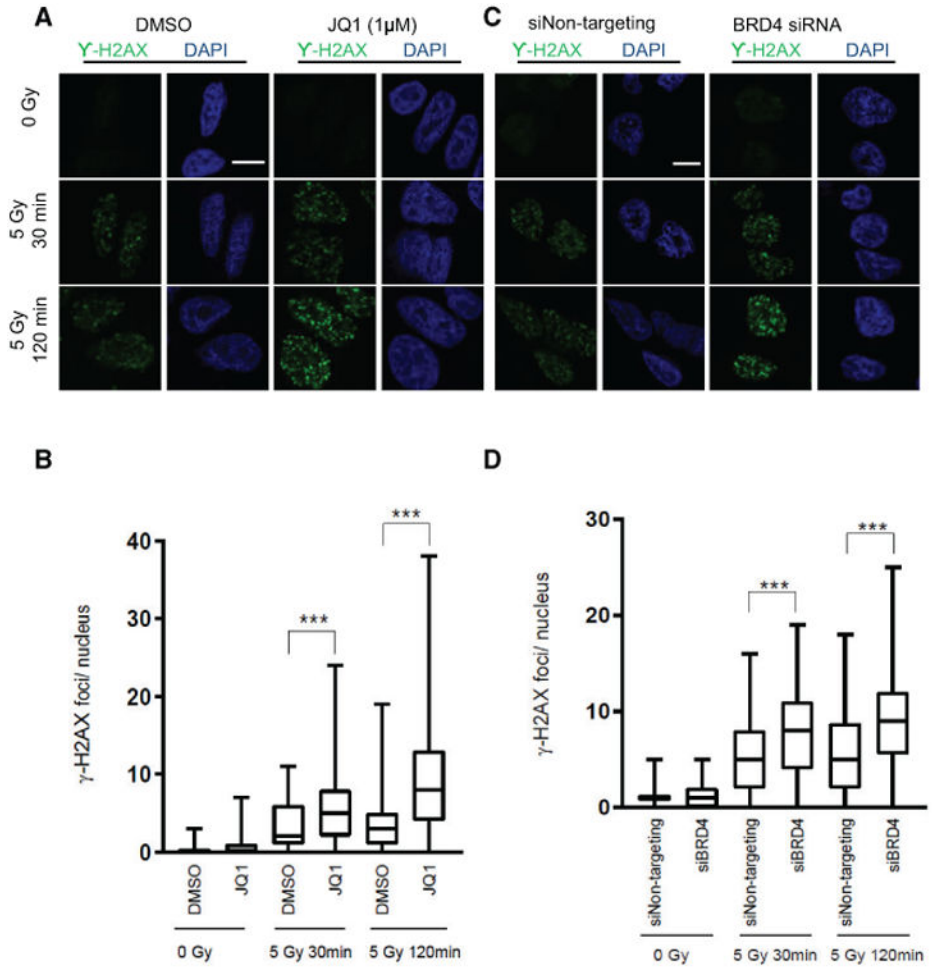

Figure 5. Loss of BRD4 Function Promotes H2AX Phosphorylation after IR Treatment

(A–D) The effect of BRD4 knockdown (A and B) or incubation with 1 μM JQ1 (C and D) in the phos-phorylation of histone H2A.X (Ser139) upon treatment of LNCaP cells with IR (5 Gy). The cells were analyzed at 30 and 120 min post-IR treatment; scale bar, 10 μm. The number of γ-H2AX foci, above threshold intensity per nucleus (n = 165) was quantified using the ImageJ software (***$p < 0.0001$ by two-tailed Mann-Whitney U test).

Author Manuscript Author Manuscript Author Manuscript Author Manuscript

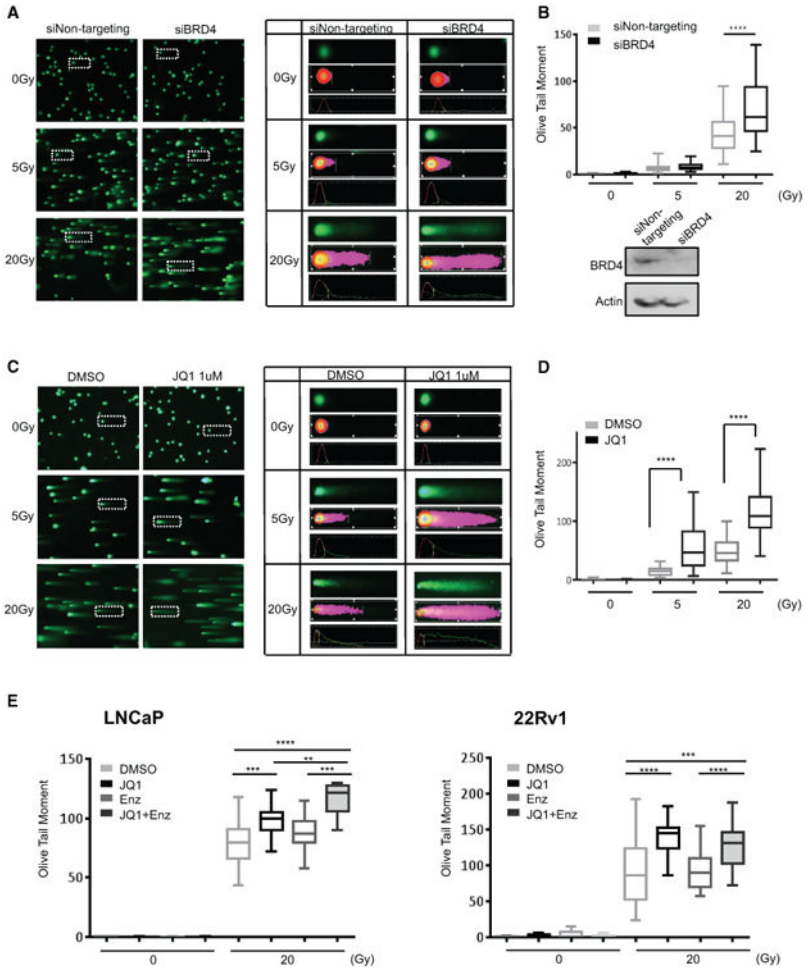

Figure 6. BRD4 Inhibition Synergizes with IR to Promote DNA Damage

(A) Alkaline comet assay of LNCaP cells with non-targeting siRNA orBRD4 siRNA, followed by treatment with the indicated doses of IR. Cells were irradiated 72-hr post-siRNA treatment, followed by recovery after 30 min.

(B) Quantification of alkaline comet assay Olive tail moment (top) and validation of BRD4 knockdown by immunoblotting (bottom).

(C) Alkaline comet assay of LNCaP cells treated with 1 μM JQ1 for 24 hr, followed by IR treatment, and recovery after 30 min.

(D) Quantification of alkaline comet assay Olive tail moment.

(E) Alkaline comet assay quantification of single-agent or combination treatment of LNCaP (left) and 22Rv1 cells (right) with 1 μM JQ1 and/or 1 μM enzalutamide for 24 hr followed by IR treatment and recovery after 30 min (**$p < 0.01$; ***$p < 0.001$; ****$p < 0.0001$ by unpaired Student's t test; error bars, SD of $n > 50$ cells fromeach sample).

Author Manuscript Author Manuscript Author Manuscript Author Manuscript

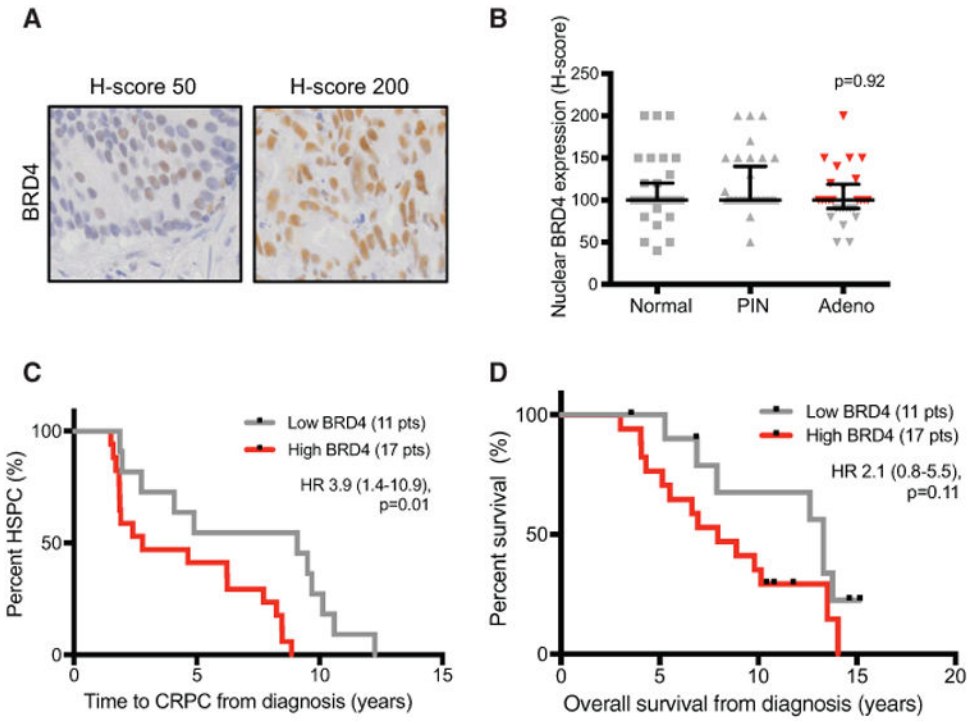

Figure 7. Nuclear BRD4 Expression Correlates with Progression to Castration Resistance PCa

(A) Representative IHC images and HS for BRD4 expression in diagnostic biopsies of prostate adenocarcinoma.

(B) Median HS and interquartile range for nuclear BRD4 expression in normal (39 patients), prostatic intraepithelial neoplasia (PIN; 37 patients), and adenocarcinoma (28 patients). Patients with adenocarcinoma were divided by BRD4 low (HS <100; 11 patients; gray) and BRD4 high (HS ≥100; 17 patients; red) for further analysis. BRD4 expression between groups was not significantly different using Kruskal-Wallis equality-of-populations rank test ($p = 0.92$).

(C and D) Kaplan-Meier curves of time to CRPC (C) (y axis represents percent hormone-sensitive PCa [HSPC]) and overall survival (D) from diagnosis after radical primary therapy are shown for low BRD4 (gray) and high BRD4 (red) groups. Hazard ratios (HRs) with 95% confidence intervals and p values for univariate cox survival model are shown.